Article

Magnesium Slag–Activated One-Part Geopolymers: A Novel Pathway Toward Low-Carbon Concrete Production

Tugba Özdemir Mazlum * and Nihat Atmaca

Posted Date: 9 December 2025

doi: 10.20944/preprints202512.0868.v1

Keywords: magnesium slag; one-part geopolymer concrete; sustainable binders; industrial byproducts; ground granulated blast furnace slag; optimal mix proportions; fresh and hardened properties; mechanical tests; microstructure analyses

 doi:10.20944/preprints202512.0868.v1

Article

Magnesium Slag–Activated One-Part Geopolymers: A Novel Pathway Toward Low-Carbon Concrete Production

Tugba Özdemir Mazlum [1,*] and Nihat Atmaca [2]

[1] Graduate School of Natural and Applied Sciences, Gaziantep University, Turkey

[2] Civil Engineering Department, Gaziantep University, Turkey

* Correspondence: ozdemir_tuuba@hotmail.com ; Tel.: +905064620772

Abstract

Amid growing environmental concerns, resource depletion, and the pressing challenges of industrial waste management, this study investigates the potential of magnesium slag (MS) as a sustainable alternative binder in the production of one-part geopolymer concretes (OPGC). The objective is to reduce reliance on conventional cementitious materials while promoting the valorization of industrial by-products in construction practices. For this purpose, ten different mixtures were designed by replacing ground granulated blast furnace slag (GGBS), the conventional aluminosilicate precursor, with MS, an innovative aluminosilicate precursor, at replacement levels of 10%, 20%, 30%, 40%, 50%, 60%, 70%, 80%, 90%, and 100% by weight, using a solid activator. The fresh and hardened properties of these mixtures were systematically evaluated through slump, setting time, density, ultrasonic pulse velocity (UPV), and strength tests, while microstructural characterization was also conducted using scanning electron microscopy (SEM) coupled with energy-dispersive X-ray spectroscopy (EDX) to further investigate the geopolymerization process, elemental distribution, and the role of MS in binder formation in OPGC. The results revealed that MS incorporation significantly influenced both workability and mechanical performance, and it was confirmed that MS actively participates in geopolymerization and can be effectively utilized up to a certain threshold. Replacement levels up to 30% were found to maintain acceptable mechanical performance, providing evidence that MS is a promising precursor for developing sustainable OPGC.

Keywords: magnesium slag; one-part geopolymer concrete; sustainable binders; industrial by-products; ground granulated blast furnace slag; optimal mix proportions; fresh and hardened properties; mechanical tests; microstructure analyses

1. Introduction

The production process of Portland cement-based concrete requires a significant amount of natural resources and contributes substantially to greenhouse gas emissions [1]. Scientists and researchers continuously explore the potential use of waste materials that can offer similar or even superior performance compared to cement-based concrete [2]. This approach aims to promote waste recycling, reduce CO_2 emissions, and conserve natural resources [3]. Over the past two decades, there has been growing interest in developing environmentally friendly construction materials by incorporating industrial by-products, such as supplementary cementitious materials or fillers. The superior performance of these materials is attributed to the morphological and pozzolanic properties of supplementary cementitious materials. These properties also play a crucial role in enhancing the structure of the cement-based concrete matrix [4].

Geopolymer concretes have emerged as a significant innovation capable of replacing Ordinary Portland Cement based concrete. By using the correct geopolymer mixture, CO_2 emissions can be reduced by up to 80% and energy consumption by up to 60% compared to conventional cement [5].

 doi:10.20944/preprints202512.0868.v1

As a result, geopolymers have gained considerable interest and recognition among researchers. The term "geopolymer" was first defined by Davidovits in 1979 [6]. Traditional geopolymer formulations typically consist of a two-component system, which includes a liquid phase (activator) and a solid phase (aluminosilicate materials). Geopolymer concretes offer numerous advantages, such as being environmentally friendly, providing high workability, and exhibiting high compressive strength [7]. They also demonstrate superior resistance to acids and sulphate [8], excellent thermal resistance [9], and low shrinkage during drying with minimal creep [10]. However, the geopolymerization process is complex and difficult to combine [11]. Additionally, there are some challenges associated with geopolymer concrete materials, such as the transportation, storage, and application difficulties of alkali solutions. These solutions are viscous, difficult to transport, and challenging to store in large quantities [12]. Since the soluble silicates used in geopolymer concrete are not entirely consumed during the geopolymerization process, this increases the permeability of conventional geopolymer concretes and reduces their durability. Therefore, the further development and improvement of two-part geopolymer concretes were necessary until the discovery of one-part geopolymer concretes.

The development of one-part geopolymer concretes has led to significant progress in the production of geopolymer concretes. These types of geopolymer concretes require only the addition of water during application. One-part geopolymer concretes consist of solid activators and alumina-silica components. These components are thoroughly mixed before use, and water is added as needed, similar to Portland cement [13]. This innovation eliminates the need for the alkaline solutions traditionally used in two-part geopolymers. Initially, some researchers identified issues such as low compressive strength [14] and poor mechanical properties [15] in one-part geopolymer concretes. However, extensive research was conducted to improve the geopolymer concretes. These studies led to increased compressive strengths of geopolymer concretes at optimal temperatures, making them competitive with traditional geopolymer concretes. Solid sodium metasilicate (Na_2SiO_3) and solid sodium hydroxide (NaOH) are highly effective powder activators in the formulation of one-part geopolymer mixtures [16]. In addition to that, some researches showed the anhydrous Na_2SiO_3 is a more effective solid activator in the metakaolin and fly ash mixture compared to the combination of hydrated Na_2SiO_3 and hydrated NaOH [17]. Also, some researches demonstrated that one-part geopolymer concrete containing a hybrid of solid Na_2SiO_3 and solid Na_2CO_3 exhibited the best overall performance in terms of mechanical performance, energy consumption, environmental impact, and economic potential [18]. A review of previous research also revealed that the performance of the innovative one-part geopolymer concrete is significantly influenced by the type of the aggregates used in the geopolymer mixtures [19].

MS is a by-product generated during the production of magnesium or ferroalloys, particularly from thermal reduction processes involving dolomite or magnesite. Chemically, MS predominantly contains magnesium oxide (MgO), calcium oxide (CaO), silicon dioxide (SiO_2), and aluminum oxide (Al_2O_3), along with smaller quantities of iron oxides and other trace elements [20]. The relatively high contents of reactive silica and alumina in MS provide potential for its use as an aluminosilicate precursor in geopolymer synthesis [21]. In addition, the presence of free lime (CaO) and periclase (MgO) may contribute to secondary hydration or carbonation reactions, which can influence setting time, dimensional stability, and mechanical performance [22]. Although MS is less reactive compared to conventional precursors like GGBS or fly ash (FA), previous studies have shown that, under alkaline activation, MS can partially participate in geopolymerization reactions and improve sustainability by reducing reliance on primary resources and mitigating waste disposal issues [23]. Nowadays, some studies have made significant attempts to conduct more comprehensive research on the CO_2 curing of MS. These investigations aim to understand the influence of carbonation parameters—such as CO_2 concentration, curing duration, and temperature—on the microstructural development, strength evolution, and carbon fixation capacity of MS-based binders. Recent findings suggest that CO_2 curing not only enhances early strength but also promotes the formation of stable carbonate phases, contributing to both durability improvement and environmental sustainability [24]. However, there is a lack of research focusing on the incorporation of MS in one-part geopolymer

 doi:10.20944/preprints202512.0868.v1

concretes. This study seeks to fill this gap in the literature by systematically examining the feasibility and performance of MS in one-part geopolymer concrete mixes.

Another type of the alumina-silicate materials used in geopolymer concrete production, GGBS, is a by-product formed during the processing of iron in the blast furnace and is an important component for geopolymer concrete due to its chemical and physical properties [25]. With its high content of reactive silica and alumina, it makes the concrete suitable for forming strong chemical bonds with alkaline activators during the geopolymerization process [26]. This process contributes to the formation of a dense and durable matrix, enabling geopolymer concrete to exhibit superior resistance to sulphate attacks, acid corrosion, and alkali-silica reactions [27]. These properties make geopolymer concrete containing GGBS an ideal material for structures exposed to harsh environmental conditions. Moreover, the low permeability of GGBS minimizes the penetration of water and harmful ions such as chlorides into the concrete matrix, thereby enhancing the long-term durability of structures [28]. The reduction in permeability of geopolymer concrete not only helps reduce environmental impacts but also lowers maintenance and repair costs [29]. In terms of mechanical performance, GGBS significantly increases the compressive strength of geopolymer concrete both in the early stages and over the long term [30]. GGBS plays a reactive role in the geopolymerization process due to its high content of calcium silicate, alumina, and other active components, contributing to the improvement of durability and mechanical properties in the concrete [31]. With its high hydraulic potential, GGBS reacts with alkaline activators to form a binder phase that strengthens the microstructure of the geopolymer matrix [32]. The use of GGBS in geopolymer concrete significantly reduces permeability, limiting the ingress of harmful ions and providing additional protection against corrosion [33]. Environmentally, the use of GGBS supports sustainability goals by reducing reliance on natural raw materials [34]. The use of GGBS as a binder in geopolymer concrete production significantly reduces the need for Portland cement, thus contributing to the reduction of carbon emissions from cement production. Additionally, utilizing industrial wastes such as MS and GGBS as a building material help mitigate waste management issues and contribute to the circular economy. Extensive research has been carried out on industrial wastes such as granulated blast furnace slag, fly ash, and steel slag, offering valuable insights into their potential reuse in traditional geopolymer concrete. Yet, studies addressing the cementitious performance of magnesium slag as a precursor in one-part geopolymer concrete are relatively limited, which contributes to its underutilization. This highlights the urgent necessity of investigating its structural properties and identifying pathways for more efficient application.

This study aimed to investigate the feasibility of utilizing MS as a precursor aluminosilicate source in one-part geopolymer concrete, in comparison with GGBS, and to determine its optimum replacement level. For this purpose, a series of fresh and hardened concrete tests were carried out on MS-based geopolymer concrete. Slump test, density and UPV (ultrasonic pulse velocity) analyses was employed to examine the workability, compactness and homogeneity of MS based geopolymer concrete, accordingly. The mechanical properties of geopolymer concrete incorporating MS at various replacement ratios with GGBS were evaluated through compressive, splitting tensile, and flexural strength tests. Furthermore, the microstructure and hydration behavior of the optimum mix containing MS were examined using scanning electron microscopy coupled with energy-dispersive X-ray spectrometry (SEM-EDX). Based on these findings, the potential and appropriate proportions of MS as an aluminosilicate precursor in one-part geopolymer concrete were discussed.

2. Experimental Program

2.1. Materials and Mix Design

MS, serving as the aluminosilicate precursor for one-part geopolymer concrete, was supplied by Kar Mineral Mining Inc., Eskişehir, Turkey. GGBS used in the experiment was provided by the Çimko Cement and Concrete Factories Inc., Gaziantep, Turkey. The chemical compositions that provided by the XRF (X-Ray fluorescence) analysis of these materials are presented in Table 1. The chemical analysis indicated that the amount of alumina (Al_2O_3) in MS is lower compared to GGBS, while the

 doi:10.20944/preprints202512.0868.v1

silica (SiO_2) contents were found to be nearly identical, recorded as 29.68% and 29.40%, respectively. In addition, the calcium (CaO) concentration in MS was reported to be higher than that in GGBS. The unit weights of the MS and GGBS used in the experiment are 2.16 and 2.86 g/cm◎ respectively. SEM microstructure images of the MS and GGBS are also demonstrated in Figure 1. The micrographs reveal notable surface irregularities and a lack of compact, dense structure, indicating heterogeneous and porous morphological characteristics.

Table 1. Chemical compositions of MS and GGBS.

Component name	MS (wt%)	GGBS (wt%)
SiO_2	29,68	29,40
Al_2O_3	1,91	15,28
Fe_2O_3	4,29	1,30
CaO	51,70	42,10
MgO	9,93	7,01
SO_3	0,52	2,87
Na_2O	0,31	0,49
K_2O	1,30	0,79
Cl	0	0,05
Loi	0,36	0,69

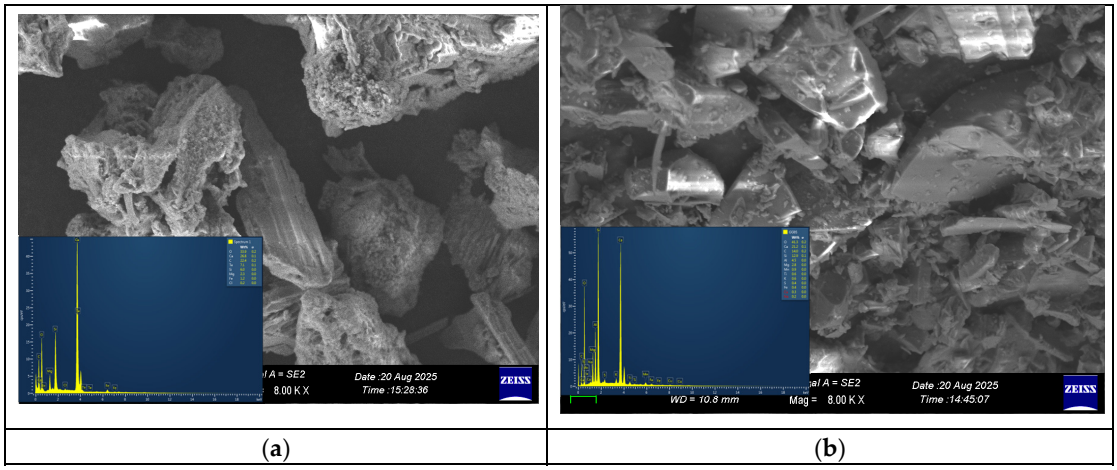

(**a**) (**b**)

Figure 1. SEM-EDX images of (**a**) MS; (**b**) GGBS.

The solid activator sodium metasilicate (Na_2SiO_3) was obtained from Songen Biotechnology and Laboratory Materials Ltd. Co., Istanbul, Turkey, and its physical and chemical properties were shown in Table 2.

Table 2. The physical and chemical properties of the solid activator sodium metasilicate.

Properties	Value
Molecular structure	Composed of Sodium (Na), Silicon (Si), and Oxygen (O) atoms
Components	Sodium Oxide (Na_2O): Provides alkaline structure Silica (SiO_2): Promotes the formation of reactive phases
Physical form	White granules
Density (solid)	2.5 g/cm◎
Solubility	Easily dissolves in water; dissociates into Na^+ and SiO_3^{2-} ions
Reactivity	Initiates the alkaline activation process Supports the formation of C-S-H and N-A-S-H gel phases in geopolymer concrete production
Moisture absorption	Rapidly absorbs moisture from the air; should be stored in a dry environment
Thermal stability	Stable up to 1088 °C

 doi:10.20944/preprints202512.0868.v1

The aggregates consist of both fine and coarse aggregate were sourced from KÇS Cement, Gaziantep, Turkey. The particle sizes of the aggregates incorporated into the concrete mixtures are within the boundaries outlined according to EN 12620 standard in Figure 2. The first category includes coarse aggregates with a maximum particle size (Dmax) of 16 mm, while the second category consists of fine aggregates with a fineness modulus of 4.37. The water absorption rates, as well as the dry and saturated surface, dry specific gravities of the aggregates used in the experiments, are presented in Table 3.

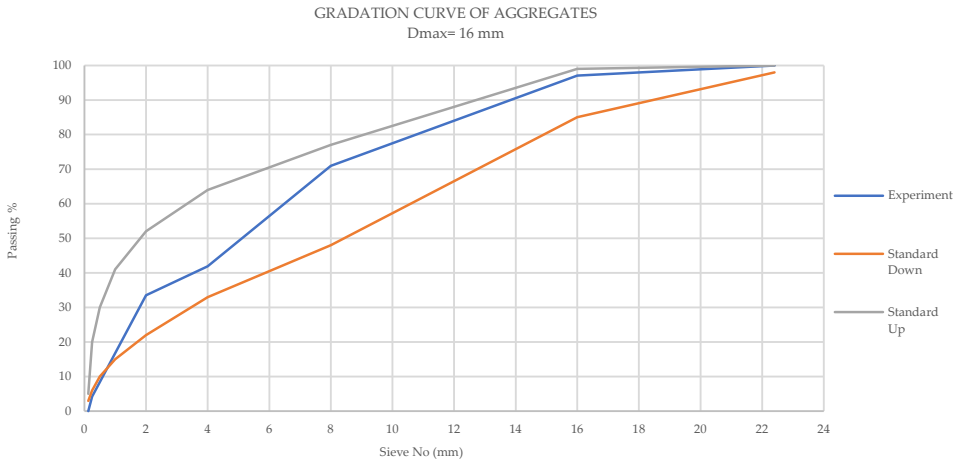

Figure 2. The gradation curve of the aggregates used in the experiment.

Table 3. The physical properties of the aggregates used in the experiment.

Properties	Value
Dry specific gravity	2,56
Saturated surface dry specific gravity	2,66
Water absorption	1,1

OPGC was produced using water, coarse-fine aggregates, and alternative cement (raw material and activator). The primary raw materials used were MS and GGBS, while solid Na_2SiO_3 was employed as the activator. Considering the similarities between conventional concrete and OPGC, the mixture design method was adapted based on previous studies [19]. The quantities used in the OPGC experiment are presented in Table 4. According to this table, the alumina-silicate materials represent MS and GGBS, while the binder consists of alumina-silicate materials and solid activator.

Table 4. The quantities of materials used in the OPGC experiment.

Materials' name	Quantities (kg/m³)
Coarse aggregate	961,0
Fine aggregate	693,0
Alumina-silicate	398,8
Binder	462,6

In this experimental OPGC mixture, the total aggregate content of the concrete was set at 70% by mass, with coarse and fine aggregates constituting 60% and 40% of the total aggregate, respectively. The ratio of solid activator to alumina-silicate materials was kept at 0,16 and the ratio of water to binder materials was kept constant as 0,47. This experimental study aims to investigate the feasibility of using MS in OPGC. Therefore, the experimental tests of each specimen were analyzed by adding MS to the GGBS based OPGC in specific proportions. In this context, MS1 represents the specimen containing 10% MS and 90% GGBS with the remaining proportions determined in a similar manner, thereby forming the table presented in the Table 5.

 doi:10.20944/preprints202512.0868.v1

Table 5. The mixture design of MS based OPGC.

	Material ID									
Materials (kg/m³)	**MS1**	**MS2**	**MS3**	**MS4**	**MS5**	**MS6**	**MS7**	**MS8**	**MS9**	**MS10**
Coarse aggregate	961,0	961,0	961,0	961,0	961,0	961,0	961,0	961,0	961,0	961,0
Fine aggregate	693,0	693,0	693,0	693,0	693,0	693,0	693,0	693,0	693,0	693,0
MS	39,9	79,8	119,6	159,5	199,4	239,3	279,2	319,0	358,9	398,8
GGBS	358,9	319,0	279,2	239,3	199,4	159,5	119,6	79,8	39,9	0,0
Activator	63,8	63,8	63,8	63,8	63,8	63,8	63,8	63,8	63,8	63,8
Water	217,4	217,4	217,4	217,4	217,4	217,4	217,4	217,4	217,4	217,4
Binder	462,6	462,6	462,6	462,6	462,6	462,6	462,6	462,6	462,6	462,6

2.2. Preparation of Specimens and Curing Conditions

A total of 270 specimens, comprising 27 from each of ten different mixes, were produced to assess the feasibility of incorporating MS into OPGC. Among these, three specimens were designated for 7-day testing and another three for 28-day testing. Each set of 7-day and 28-day specimens included one cube, one cylinder, and one prism type, with three identical specimens cast for each to allow for averaging the results. The mixing process was carried out a laboratory-scale pan mixer with a 75-liter capacity and a rotational speed of 280 rpm. Initially, the coarse and fine aggregates were dry-mixed for approximately 2 minutes. Subsequently, the MS and GGBS was added to the mixture, and mixing continued for another 2 minutes to ensure uniform distribution of the dry materials. Once a consistent dry mix was achieved, the solid activator was introduced by dissolving in the mixing water for enhancing the homogeneity of the mixture and ensuring better penetration of the activator into the other solid constituents as shown in Figure 3. The mixture was then blended for an additional 6 minutes until a uniform consistency was obtained. Slump tests were carried out directly after mixing, in accordance with EN 12350-2, to evaluate the workability of the fresh concrete mixtures. The test was conducted under ambient temperature conditions of 20 ± 2 °C. The final fresh mixture, which followed a process similar to conventional concrete production and thus offers practical advantages in terms of ease of handling, was cast into molds (oiled before use) for experimental testing. Cube specimens (150×150×150 mm), cylindrical specimens (100×200 mm), and prism specimens (100×100×400 mm) were prepared accordingly. After casting into the molds, the specimens were compacted with the aid of a vibrator to ensure proper consolidation and eliminate entrapped air. After casting and vibrating, the specimens were covered with heat-resistant plastic wrap to prevent moisture loss and then placed in a furnace set at 60 °C for thermal curing. The purpose of this process was to accelerate the chemical reactions among the constituents of the geopolymer concrete, thereby ensuring timely setting. As part of the preliminary study, specimens without thermal curing were also prepared. It was observed that these specimens exhibited delayed setting, and those demolded prematurely lost their structural integrity. Therefore, thermal curing was deemed essential for the proper setting of one-part geopolymer concrete. The specimens remained in the furnace for 24 hours. Upon completion of thermal curing, they were removed from the furnace, the plastic wrap was taken off, and the specimens were sealed in plastic bags to retain their internal moisture. They were then stored at ambient temperature until the designated testing days.

2.3. Testing Method

The slump test was performed to assess the workability of fresh OPGC mixtures as seen in Figure 4.a. The test followed EN 12350-2 standard procedures and was conducted immediately after mixing. The primary objective was to evaluate the consistency and flow behavior of the mixtures containing varying proportions of MS and GGBS. Due to the absence of Portland cement and the unique setting characteristics of geopolymer systems, fresh-state behavior can differ significantly

 doi:10.20944/preprints202512.0868.v1

from conventional concrete. Therefore, the slump test served as an essential indicator to determine whether the mixtures had adequate flowability for proper casting and compaction. The results provided valuable insight for optimizing mix proportions in relation to fresh concrete performance.

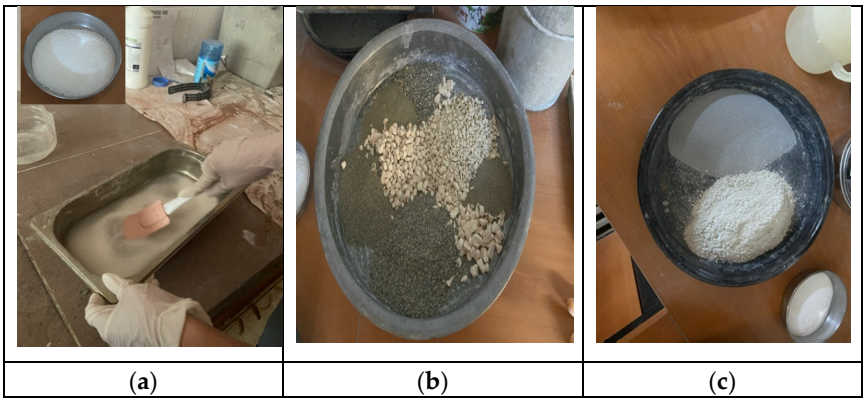

Figure 3. Mixing and curing stages of MS based OPGC **a.** dissolving of solid activator in the water, **b.** coarse and fine aggregates, **c.** MS (up) and GGBS (bottom) used for experiment.

The setting time of MS-based OPGC were determined in accordance with ASTM C807-21 standard as seen in Figure 4.b. For this purpose, mortar was obtained by sieving fresh concrete through a #4 mesh to remove coarse aggregates. The setting time was recorded from the moment the aluminosilicate materials came into contact with the activator until penetration of a 2 mm diameter needle was less than 10 mm. The reported values for setting time were derived from the average of two specimens.

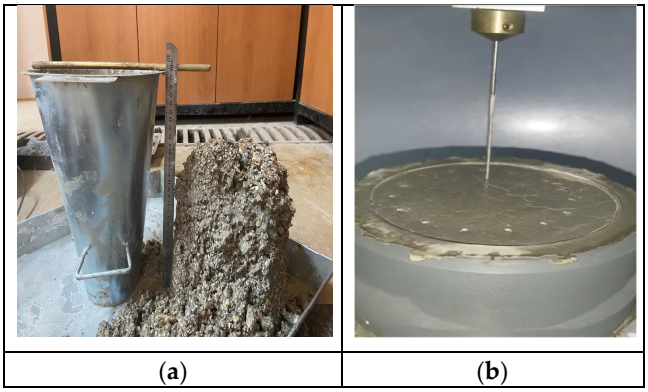

Figure 4. Experimental test procedures of fresh MS-based OPGC: **(a)** Slump test; **(b)** Determination of setting time.

The density of hardened OPGC was determined to evaluate the compactness and uniformity of the specimens in accordance with EN 12390-7 standard. After 28 days of curing, cubic samples were dried to a constant weight and their mass and volume were recorded as seen in Figure 5.a. The density was calculated by dividing the mass of the specimen by its volume, following standard procedures. This simple but important measurement provides insight into the internal structure of the concrete, indicating the degree of compaction and potential presence of voids. A consistent and relatively high density value suggests effective particle packing and good quality in the hardened state.

 doi:10.20944/preprints202512.0868.v1

(a) (b) (c) (d) (e)

Figure 5. Experimental test procedures of hardened MS based OPGC: **(a)** Measurement of specimen weight for density determination; **(b)** Ultrasonic pulse velocity (UPV) test; **(c)** Compressive strength test on cube specimen; **(d)** Splitting tensile strength test on cylindrical specimen; **(e)** Flexural strength test on prismatic specimen.

The ultrasonic pulse velocity (UPV) test was carried out on 28-day cured OPGC specimens to assess their internal quality in a non-destructive manner. The test was conducted in accordance with EN 12504-4 standard using a portable UPV device equipped with two transducers. A coupling gel was applied to the surface of the specimens to ensure proper contact and signal transmission. The transducers were positioned on opposite faces of the concrete sample as seen in Figure 5.b, and the time taken for the ultrasonic pulse to travel through the material was recorded. The pulse velocity was calculated by dividing the specimen length by the travel time. Higher pulse velocities generally indicate a denser and more homogeneous structure, while lower values may suggest internal flaws, voids, or microcracks.

The compressive strength of the concrete cube specimens (150×150×150 mm) was determined in accordance with EN 12390-3 standard. Prior to testing, the surface of each specimen was cleaned and aligned carefully to ensure uniform load distribution during testing. A calibrated compression testing machine as seen in Figure 5.c with a capacity of 2000 kN was used to apply the load at a constant pace rate of approximately 0.6 MPa/s until failure. The average value of three specimens was recorded as the compressive strength for each mix design at early age strength as 7-days, at standard age strength as 28-days, and long-term strength as 90 days.

The splitting tensile strength of concrete specimens was determined in accordance with EN 12390-6 standard. The cylindrical specimens, with dimensions of 100×200 mm, were placed horizontally between the loading platens of the testing machine as seen in Figure 5.d. A compressive load was applied along the vertical diameter of each specimen using strips to ensure uniform stress distribution. The load was applied at a constant rate of 0.05 MPa/s until failure occurred. The maximum load at failure was recorded, and the splitting tensile strength was calculated accordingly. The tests were performed at 28-days of curing, and the average value of three specimens was reported for each age.

The flexural strength of prism specimens (100×100×400 mm) was assessed following the third-point loading method specified in EN 12390-5. Specimens were positioned on two supporting rollers spaced 30 cm apart, and the load was applied through two loading rollers placed symmetrically at one-third span points as seen in Figure 5.e. The test was conducted using a universal testing machine at a loading rate of 0.1 MPa/s until failure occurred with 28-days of curing specimens. The flexural strength was calculated based on the maximum load and span dimensions, and the average of three specimens was taken as the representative value.

In the final stage, SEM (Scanning Electron Microscopy) and EDX (Energy Dispersive X-ray Spectroscopy) analyses were carried out to examine the microstructural and chemical characteristics of the specimens. The SEM analysis provided high-resolution images of the surface morphology and pore structure, offering detailed insights into the distribution of hydration products, microcracks, and bonding zones. In this study, the SEM device used was the Zeiss Gemini SEM 300. Furthermore, with the aid of the EDX detector integrated into the SEM system, the elemental composition of the

 doi:10.20944/preprints202512.0868.v1

material was identified; in particular, the distribution and proportions of elements such as Si, Al, Ca, Mg, and Fe—which play a critical role in the geopolymerization process—were determined. Thus, a comprehensive assessment was achieved from both morphological and chemical perspectives, clearly revealing the influence of the raw materials (MS and GGBS) on the formation of reaction products.

3. Results and Discussion

3.1. Workability

Table 6 shows the workability results of MS-based OPGC. All mixtures exhibited a satisfactory level of workability. In general, the mixtures exhibited similar slump values, but workability showed an upward trend increasing the proportion of MS. This situation is explained by the mineralogical composition of magnesium slag. It mainly consists of quartz, larnite, calcium silicate, periclase, and calcio-olivine [35]. The silicon present in MS is largely in the form of Q^0 and Q^4 units, which are associated with a high number of bridging oxygens and a strong degree of [SiO_4] polymerization. This structural characteristic results in relatively lower inherent cementitious activity compared to the GGBS, where silicon is predominantly present in Q^0 units with fewer bridging oxygens and a lower polymerization degree, providing higher reactivity. However, when exposed to alkali activation, the latent cementitious potential of MS becomes more evident, although still significantly lower than that of GGBS. This microstructural behavior explains why mixtures with higher MS content show improved workability despite their lower cementitious reactivity.

Table 6. The mixture design of MS based OPGC.

Material ID	Slump value (cm)	MS value (%)	GGBS value (%)
MS1	7	10	90
MS2	8	20	80
MS3	8	30	70
MS4	9	40	60
MS5	10	50	50
MS6	10	60	40
MS7	11	70	30
MS8	12	80	20
MS9	12	90	10
MS10	14	100	0

3.2. Setting Time

The initial and final setting times results of MS-based GGBS are shown in Figure 6. The initial and final setting times increased progressively with the rise in MS content. In the MS1–MS3 range, the initial setting occurred within approximately 100–150 minutes, indicating a relatively rapid hardening behavior. From MS6 onwards, a marked increase in setting times was observed, with the final setting of MS10 reaching 600 minutes. It has been shown that MS markedly extend the setting time in geopolymer systems. This trend is attributed to the comparatively slower dissolution and reaction rate of MS [36] and the fact that GGBS-based systems accelerate the reaction kinetics [37]. According to this graph in Figure 6, when the GGBS was 90% replaced by MS, the duration of the initial and final set was extended from 95 to 480 min (405%) and 140 to 600 min (320%), respectively. This aligns with earlier studies indicating that increasing the proportion of GGBS in the binder leads to a reduction in setting time [38–40]. It also agrees with the initial and final setting times reported in other studies [41].

 doi:10.20944/preprints202512.0868.v1

Overall, the general tendency was that higher MS replacement resulted in longer setting times, whereas lower MS levels led to shorter setting times.

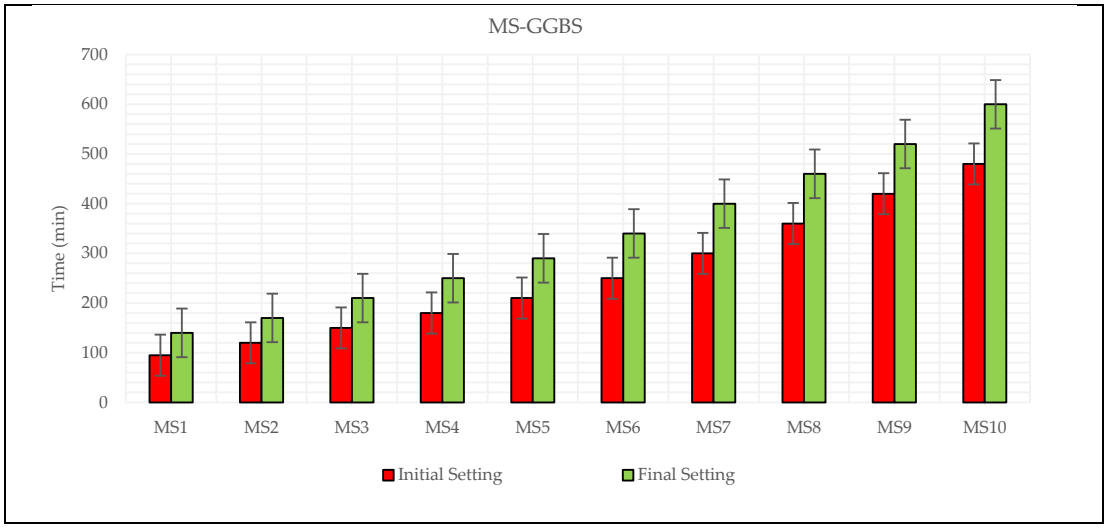

Figure 6. Initial and final setting times of MS-based OPGC.

3.3. Wet Apparent Density

The wet apparent density of each mixture was measured at 28 days prior to conducting the UPV and strength tests. The results revealed that the density of OPGC mixtures decreased progressively with increasing MS content. As shown in Figure 7, mixtures incorporating 10% MS measured the highest density (2.28 g/cm◉), whereas those with 100% MS reached the lowest value (2.10 g/cm◉). The observed decrease in density is attributed to the adverse effect of MS on the particle size distribution within the mixture [42]. This condition hindered the dense and efficient packing of particles, leading to an increase in the void sizes within the geopolymer concrete mixture. Compared to GGBS that is more reactive and denser binder, MS contributes to a reduced overall density [43]. As a result, the mixture containing 10% MS was denser by about 7.9% compared to the mixture incorporating 100% MS.

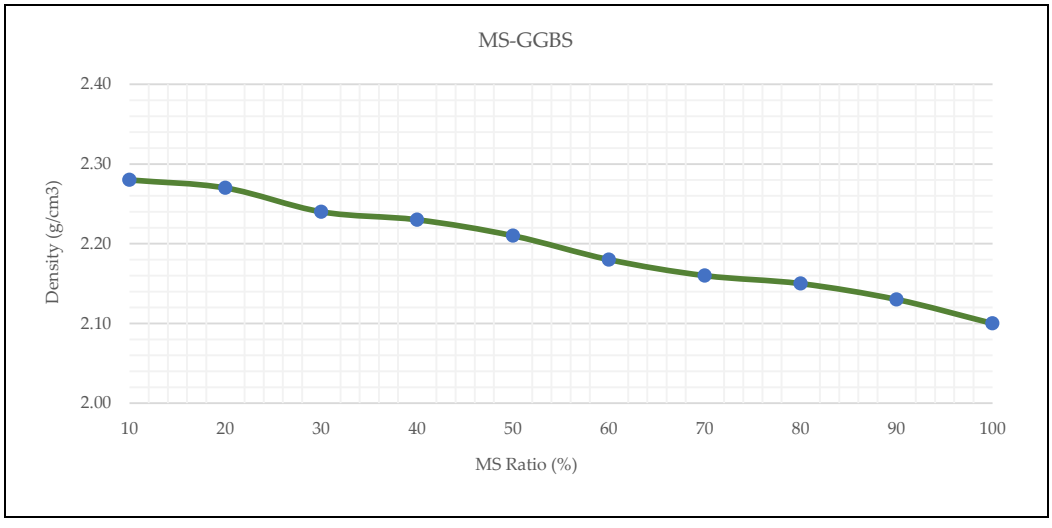

Figure 7. Wet apparent density results of MS-based OPGC.

Moreover, the slump–density curve presented in Figure 8 revealed an inverse relationship between these two parameters. Mixtures with higher densities (≥2.27 g/cm◉) exhibited lower slump

 doi:10.20944/preprints202512.0868.v1

values (7–8 cm), indicating stiffer and less workable mixes. On the other hand, as density decreased, slump values increased, with the most fluid mixture (100% MS) reaching a slump value of 14 cm. However, this increased flowability did not reflect improved quality; instead, it indicated the presence of excessive free water and entrapped air due to insufficient reactivity and lack of cohesion. These findings demonstrate that both excessively high and low MS contents can negatively affect the fresh performance of geopolymer concrete. Therefore, maintaining a balanced ratio of MS and GGBS is essential to achieve optimal density and workability, which are critical for the production of durable and structurally sound geopolymer concretes.

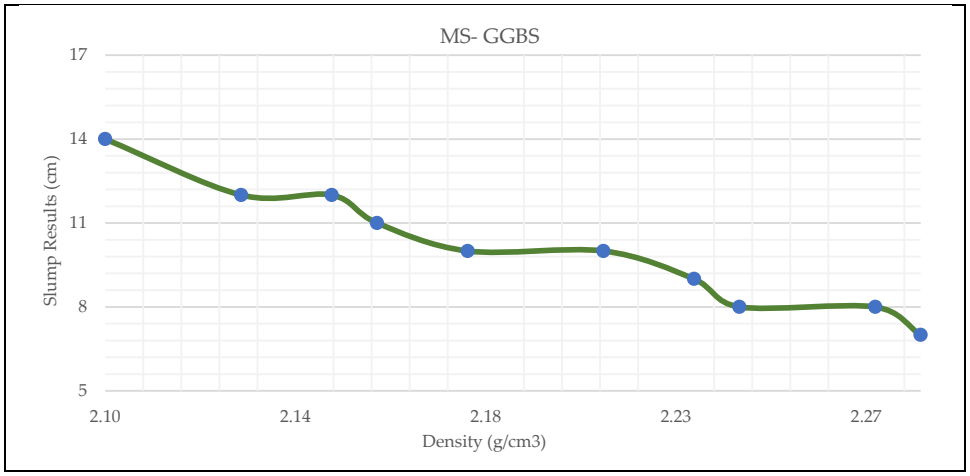

Figure 8. Slump test results vs wet apparent density results.

3.4. Ultrasonic Pulse Velocity (UPV)

The UPV test of each mixture was measured at 28 days prior to conducting strength tests. The UPV test results show a clear decrease as the MS ratio increases in the OPGC mixtures. As shown in the Figure 7, UPV values dropped from 3420 m/s at 10% MS to 3150 m/s at 100% MS, reflecting a gradual loss in ultrasonic wave transmission capacity through the material matrix. This reduction in UPV is attributed to the porous nature and lower compactness of magnesium slag when used in higher proportions [44]. Compared to more reactive and denser materials like GGBS, MS tends to form less cohesive and more voided structures, which disrupt the continuity of the solid matrix and slow down wave propagation [45]. In geopolymer systems, high UPV values generally correlate with good microstructural integrity, low porosity, and strong inter-particle bonding. Therefore, the observed decline in UPV suggests that increasing MS content leads to weaker internal structure, increased micro-voids, and reduced bonding quality.

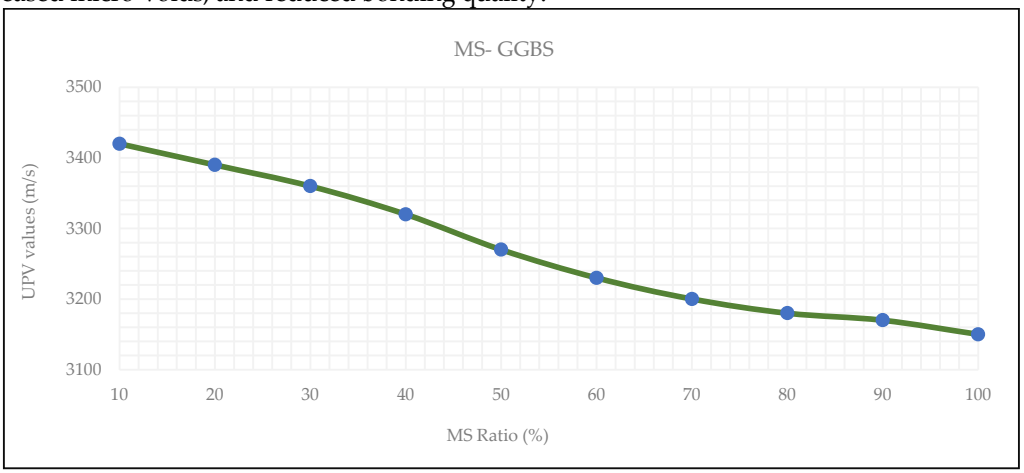

Figure 7. UPV test results of MS-based OPGC.

 doi:10.20944/preprints202512.0868.v1

3.5. Compressive Strength

The compressive strength test results of MS-based OPGC mixtures are illustrated in Figure 8. Each value presented represents the average of at least three tested specimens. The obtained results indicate that the proportion of MS in the OPGC mixtures played a crucial role in the development of compressive strength. The 7-day strength of the samples ranged from 1.20 to 62.78 MPa, the 28-day strength varied between 3.60 and 72.53 MPa, and the 90-day strength ranged from 5.30 to 75.48 MPa as seen in Figure 8. The highest compressive strength was recorded for the mixture incorporating 10% MS, which exhibited strength characteristics comparable to those of high-performance conventional concretes. As shown in Figure 8, increasing the MS content from 10% to 100% progressively reduced the compressive strength at all curing ages (7, 28, and 90 days).

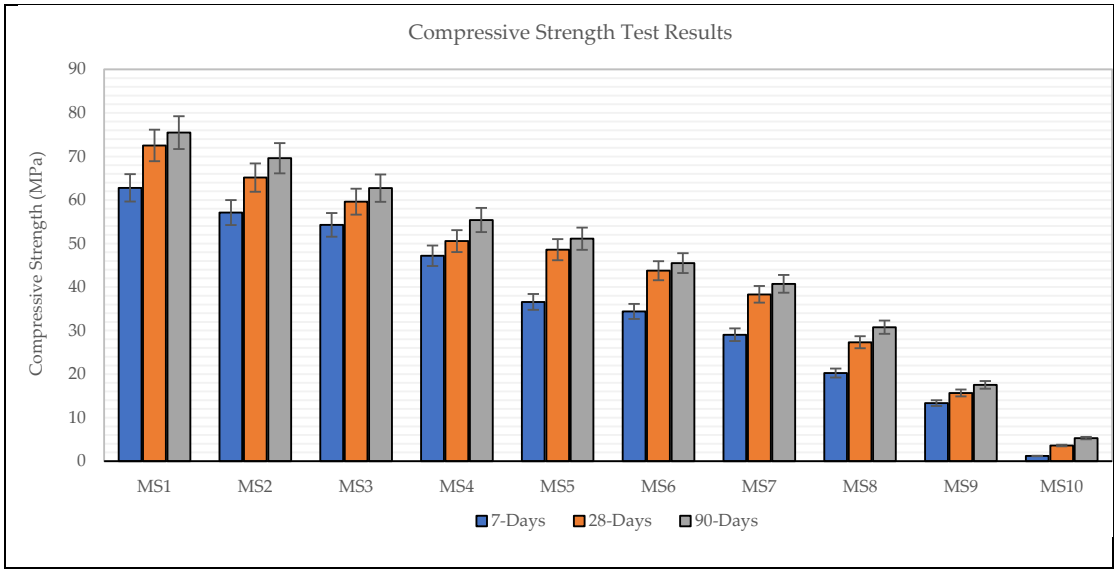

Figure 8. Compressive strength test results of MS-based OPGC.

The geopolymerization process begins with the decomposition of solid aluminosilicate materials into silicate and aluminate monomers, which subsequently undergo condensation reactions to form the geopolymer gel. Moreover, an increased calcium content in geopolymer concrete has been reported to facilitate the dissolution of aluminosilicates by elevating the pH of the surrounding medium, thereby enhancing the degree of geopolymerization and promoting the development of a stronger geopolymer network [43]. The rise in compressive strength resulting from the reduction of MS content can be linked to the balanced effect of soluble silica originating from both the activator and GGBS. This interaction enhances the strength development at different curing ages. In contrast, mixes composed solely of MS (100% MS) demonstrated restricted strength gain, as verified by these experimental findings. Additionally, the gradual improvement in strength could be related to the chemical reaction between aluminosilicate phases and the solid activator, which facilitates the dissolution of silica and alumina and accelerates the geopolymerization mechanism [46]. When the MS content reached 30%, the overall silica and alumina concentration in the binder matrix decreased rapidly due to the nature of MS. Consequently, the number of Si–O–Al bonds, especially between MS and GGBS particles, was reduced, leading to a drop in compressive strength. Moreover, the relatively low strength of the mixtures containing 100% MS can be attributed to the insufficient calcium content, which limits the dissolution and subsequent gel formation [47].

It is noteworthy that the obtained results are consistent with previous findings [48,49] in which researchers investigated the influence of MS in traditional concrete. Moreover, Figure 9 shows the fractured specimens of hardened concrete after compressive strength test.

 doi:10.20944/preprints202512.0868.v1

Figure 9. Fractured specimens of hardened concrete after compressive strength test.

3.6. Splitting Tensile Strength

The results illustrated in Figure 10 show a clear inverse relationship between the MS content and the 28-day splitting tensile strength of OPGC mixtures. As the MS replacement ratio increased from 10% to 100%, the splitting tensile strength consistently decreased, dropping from 4.89 MPa at MS10 to 1.22 MPa at MS100. This decline parallels the trend observed in compressive strength, indicating that higher MS content not only weakens the matrix in compression but also compromises its tensile integrity. The reduction in tensile strength is attributed to the limited reactivity and poor gel formation ability of MS compared to more reactive binders like GGBS. With increasing MS content, the geopolymer matrix likely contains more internal voids and exhibits weaker inter-particle bonding, leading to a brittle failure under tensile stress. The steep decline after 50% MS further supports the conclusion that excessive MS content disrupts cohesive strength development within the binder phase.

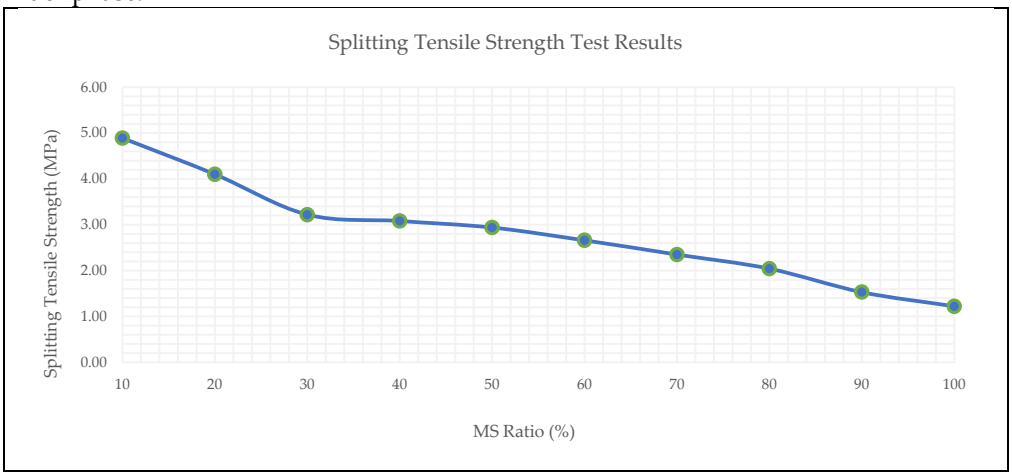

Figure 10. Splitting tensile strength test results of MS based OPGC.

Overall, these results suggest that high MS contents significantly reduce the tensile performance of OPGC, and that the material becomes unsuitable for structural applications requiring adequate tensile resistance. It reinforces the recommendation that MS should be used at replacement levels not exceeding 30% to maintain acceptable mechanical properties as clarified in previous studies [50].

3.7. Flexural Strength

The experimental results presented in Figure 11 illustrate the influence of MS content on the 28-day flexural strength of OPGC. A consistent downward trend was observed in the mechanical properties as the MS replacement ratio increased from 10% to 100%.

 doi:10.20944/preprints202512.0868.v1

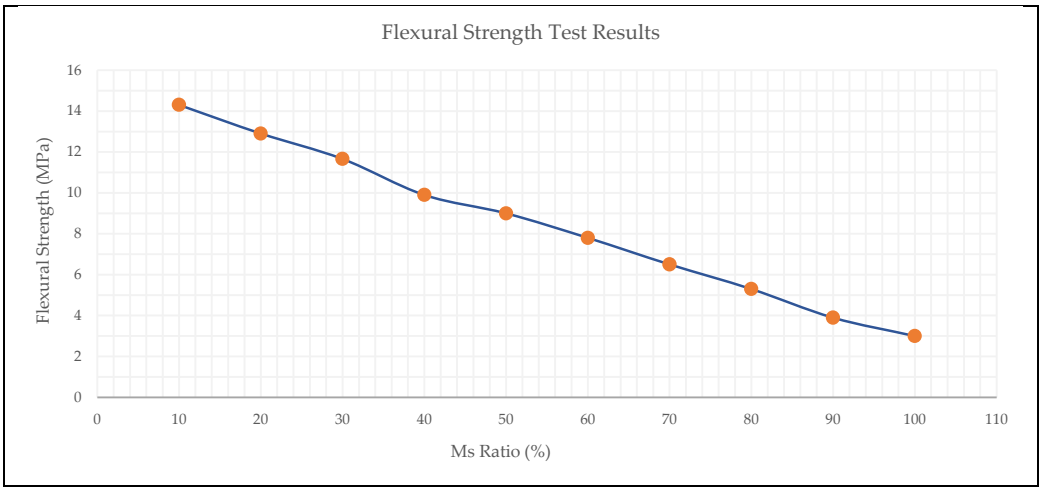

Figure 11. Splitting tensile strength test results of MS based OPGC.

Mixtures containing lower MS ratios (10–30%) exhibited superior flexural performance, reaching a maximum of 14.30 MPa at 10% MS, followed by 12.90 MPa and 11.66 MPa for 20% and 30% MS, respectively. Beyond this threshold, the flexural strength progressively declined. This behavior is attributed to the lower reactivity and gel-forming capacity of MS compared to GGBS, which limits the development of a dense and cohesive microstructure essential for flexural load resistance. The comparison graph Figure 12 clearly highlights that flexural strength consistently exceeds splitting tensile strength across all mix compositions, with the gap widening at lower MS contents. This suggests that while both properties degrade with increasing MS, flexural behavior remains more resilient, due to its dependence on both matrix quality and aggregate bridging mechanisms [51]. These findings confirm that excessive MS replacement adversely impacts the tensile-related mechanical properties of OPGC. To maintain structural performance within acceptable limits, the MS content should be limited to 30% or below, especially in applications where flexural or tensile stresses are critical.

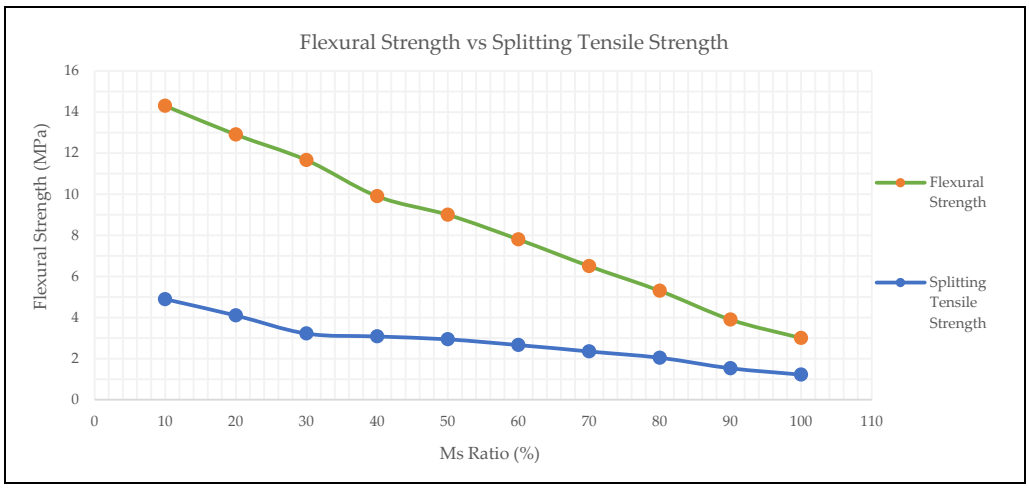

Figure 12. Comparison of 28-day flexural and splitting tensile strengths of MS based OPGC.

3.8. Scanning Electron Microscopy (SEM)

Three selected one-part geopolymer concrete samples containing 30%, 40%, and 50% MS and solid activators, cured at 60 °C for 24 hours, were examined using SEM to investigate their morphology and microstructure. The results of this analysis are presented in Figure 13. The SEM images were analyzed to gain a clearer understanding of the microstructural characteristics and

 doi:10.20944/preprints202512.0868.v1

morphology of the formed geopolymer. As shown in Figure 13.a, e MS30 specimen exhibited a dense and compact matrix with very limited unreacted particles and microcracks. The homogeneously distributed reaction products indicate a well-developed geopolymer network. This microstructure suggests that the high calcium content of GGBS contributed to the formation of C–A–S–H and N–A–S–H gels, which are known to enhance matrix cohesion and strength [52]. Similar compact morphologies have been linked in the literature to higher compressive strength and lower porosity [28,53].

The MS40 specimen displayed a partially compact yet fibrous and layered microstructure as shown in Figure 13.b. The presence of these fibrous gel formations may indicate a slower dissolution of aluminosilicate species due to the increased MS content, leading to heterogeneity in the reaction products. Previous studies [54,55] have also reported that higher proportions of MS can decrease reactivity, resulting in localized microcrack formation and less uniform gel distribution. The coexistence of dense and porous regions observed here supports this explanation.

In the MS50 sample, microcracks and porous regions became more pronounced as seen in Figure 13.c. Several unreacted MS particles were clearly visible, suggesting incomplete geopolymerization. The reduction in calcium availability and the slower dissolution rate of MS likely limited the formation of binding gels, producing a weaker and more discontinuous matrix. These microstructural features correspond well with the observed reduction in compressive strength, consistent with earlier findings by [21,56].

Overall, as the MS content increased, the reactive Si and Al species available for geopolymerization decreased, leading to reduced gel formation and a less cohesive structure. Mixtures with up to 30% MS exhibited a dense, homogeneous matrix, while those with 50% MS displayed a heterogeneous and crack-prone morphology. This trend aligns with previous reports suggesting that maintaining MS content below 30% ensures adequate reactivity and mechanical performance [21,48].

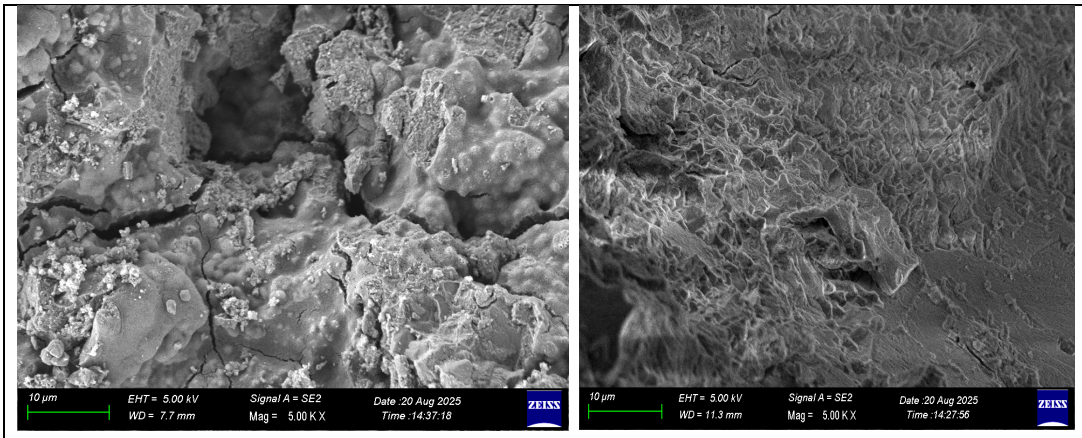

(a) **(b)**

 doi:10.20944/preprints202512.0868.v1

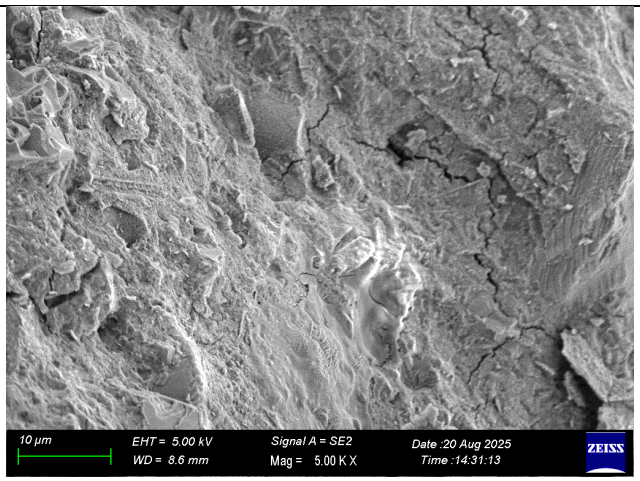

(c)

Figure 13. SEM micrograph of **(a)** 30% MS based OPGC **b)** 40% MS based OPGC, **(c)** 50% MS based OPGC.

4. Discussion

Based on the comprehensive experimental investigation, it can be concluded that MS exhibits limited potential as a sole precursor in OPGC systems due to its inherently low reactivity, poor binding characteristics, and inadequate gel-forming ability. The use of 100% MS resulted in poor workability, low density, weak mechanical strength, and insufficient setting behavior, all of which highlight its unsuitability for standalone use. However, when MS was blended with GGBS, especially at replacement levels of 30% or below, the resulting OPGC mixtures demonstrated improved performance in terms of workability, density, and mechanical properties. The synergy between MS and GGBS, particularly under optimal water-to-binder ratios, facilitated the formation of a denser and more cohesive matrix with sufficient strength development. Therefore, MS can be considered a viable supplementary precursor in OPGC systems when used in moderate proportions alongside more reactive binders. Taking all performance criteria into account, including workability, setting behavior, strength, and microstructure; an MS replacement level of 30% or less is identified as the optimum range for OPGC systems.

Beyond its role in mechanical performance, the incorporation of MS into OPGC mixtures offers significant environmental benefits. MS is an industrial by-product generated in large quantities from magnesium production processes, and its disposal often poses environmental challenges, including land occupation and potential groundwater contamination. Utilizing MS in OPGC as a partial replacement for traditional binders such as GGBS contributes to waste valorization, reduces the environmental footprint of concrete production, and aligns with circular economy principles.

Author Contributions: Conceptualization, Tuğba Özdemir Mazlum, Nihat Atmaca; methodology, Tuğba Özdemir Mazlum, Nihat Atmaca; validation, Tuğba Özdemir Mazlum, Nihat Atmaca; formal analysis, Nihat Atmaca; investigation, Tuğba Özdemir Mazlum.; resources, Tuğba Özdemir Mazlum, Nihat Atmaca.; data curation, Tuğba Özdemir Mazlum; writing—original draft preparation, Tuğba Özdemir Mazlum.; writing—review and editing, Nihat Atmaca; supervision, Nihat Atmaca; funding acquisition, Nihat Atmaca. All authors have read and agreed to the published version of the manuscript.

Funding: This research was funded by Scientific Research Projects Programme of Gaziantep University under Project No: MF. HZP. 24. 13., and YOK 100/2000 fellowship of government.

Institutional Review Board Statement: Not applicable.

Data Availability Statement: Data will be made available on request.

 doi:10.20944/preprints202512.0868.v1

Acknowledgments: The authors would like to express their sincere gratitude to Kar Mineral Mining Inc. for supplying the magnesium slag used in this study and to Songen Biotechnology and Laboratory Materials Ltd. Co. for providing the solid activator. Special thanks are also extended to KÇS Cement (Turkey) for supplying the aggregates used in the experiments. Furthermore, the authors gratefully acknowledge the financial support provided by the Scientific Research Projects Programme of Gaziantep University under Project No: MF. HZP. 24. 13., and YOK 100/2000 fellowship of government which enabled the mobility of the researchers and contributed to the successful execution of this research.

Conflicts of Interest: The authors declare no conflicts of interest.

Abbreviations

The following abbreviations are used in this manuscript:

MS	Magnesium Slag
OPGC	One Part Geopolymer Concrete
GGBS	Ground Granulated Blast Furnace Slag
UPV	Ultrasonic Pulse Velocity

References

1. El-Mir, A., Hwalla, J., El-Hassan, H., Assaad, J. J., El-Dieb, A., Shehab, E. Valorization of waste perlite powder in geopolymer composites. *Construction and Building Materials*, 2023, 368, 130491.
2. Guo, S., Ma, C., Long, G., Xie, Y., Cleaner one-part geopolymer prepared by introducing fly ash sinking spherical beads: properties and geopolymerization mechanism, *Journal of Cleaner Production*, 2019, 219, 686–697.
3. Sumesh, M., Alengaram, U. J., Jumaat, M. Z., Mo, K. H., Alnahhal, M. F., Incorporation of nano-materials in cement composite and geopolymer based paste and mortar–A review, *Construction and Building Materials*, 2017, 148, 62–84.
4. Meng, Y., Ling, T. C., Mo, K. H., Recycling of wastes for value-added applications in concrete blocks: An overview, *Resources, Conservation and Recycling*, 2018, 138, 298–312.
5. Oderji, S. Y., Chen, B., Ahmad, M. R., Shah, S. F. A., Fresh and hardened properties of one-part fly ash-based geopolymer binders cured at room temperature: Effect of slag and alkali activators, *Journal of Cleaner Production*, 2019, 225, 1–10.
6. Pacheco-Torgal, F., Introduction to handbook of alkali-activated cements, mortars and concretes, In: Handbook of alkali-activated cements, mortars and concretes, 2015, pp. 1–16, Woodhead Publishing.
7. Zhang, Y. J., Wang, Y. C., Li, S., Mechanical performance and hydration mechanism of geopolymer composite reinforced by resin, *Materials Science and Engineering*, 2010, 527(24-25), 6574–6580.
8. Aiken, T. A., Kwasny, J., Sha, W., Soutsos, M. N., Effect of slag content and activator dosage on the resistance of fly ash geopolymer binders to sulfuric acid attack, *Cement and Concrete Research*, 2018, 111, 23–40.
9. Yao, X., Zhang, Z., Zhu, H., Chen, Y., Geopolymerization process of alkali–metakaolinite characterized by isothermal calorimetry, *Thermochimica Acta*, 2009, 493(1-2), 49–54.
10. Sagoe-Crentsil, K., Brown, T., Taylor, A., Drying shrinkage and creep performance of geopolymer concrete, *Journal of Sustainable Cement-Based Materials*, 2013, 2(1), 35–42.
11. Kong, D. L., Sanjayan, J. G., Effect of elevated temperatures on geopolymer paste, mortar and concrete, *Cement and Concrete Research*, 2010, 40(2), 334–339.
12. Luukkonen, T., Abdollahnejad, Z., Yliniemi, J., Kinnunen, P., Illikainen, M., Comparison of alkali and silica sources in one-part alkali-activated blast furnace slag mortar, *Journal of Cleaner Production*, 2018, 187, 171–179.
13. Abdel-Gawwad, H. A., Rashad, A. M., Heikal, M., Sustainable utilization of pre-treated concrete waste in the production of one-part alkali-activated cement, *Journal of Cleaner Production*, 2019, 232, 318–328.

 doi:10.20944/preprints202512.0868.v1

14. Koloušek, D., Brus, J., Urbanova, M., Andertova, J., Hulinsky, V., Vorel, J., Preparation, structure and hydrothermal stability of alternative (sodium silicate-free) geopolymers, *Journal of Materials Science*, 2007, 42, 9267–9275.
15. Peng, M. X., Wang, Z. H., Shen, S. H., Xiao, Q. G., 2015. Synthesis, characterization and mechanisms of one-part geopolymeric cement by calcining low-quality kaolin with alkali, *Materials and Structures*, 48, 699–708.
16. Ma, C., Long, G., Shi, Y., Xie, Y., 2018. Preparation of cleaner one-part geopolymer by investigating different types of commercial sodium metasilicate in China, *Journal of Cleaner Production*, 201, 636–647.
17. Zhang, T., Zhang, Y., He, Y., Zhao, Y. and Shi, C., 2022. Alkali-activated materials from metakaolin and MSW incineration fly ash: Reaction kinetics and microstructure. *Cement and Concrete Composites*, 130, p.104483.
18. Lao, J. C., Xu, L. Y., Huang, B. T., Zhu, J. X., Khan, M., Dai, J. G., 2023. Utilization of sodium carbonate activator in strain-hardening ultra-high-performance geopolymer concrete, *Frontiers in Materials*, 10, 1142237.
19. Alhamoud, A., Tajmir Riahi, H., Ataei, A., 2024. A Practical Mix Design Method of Ground Granulated Blast-Furnace Slag-Based One-Part Geopolymer Concrete, *Arab Journal Science and Engineering*, 49, 5447–5466.
20. Lu, P., Zhao, Y., Zhang, N., Wang, Y., Zhang, J., Zhang, Y., and Liu, X., Structural characteristics and cementitious behavior of magnesium slag in comparison with granulated blast furnace slag. *Materials*, 2024, *17*(2), 360.
21. Kumar, S., Kumar, R. and Mehrotra, S.P., Influence of granulated blast furnace slag on the reaction, structure and properties of fly ash-based geopolymer. Journal of Materials Science, 2017, 52(5), pp.2618–2630.
22. Frías, M., Moreno-Reyes, A. M., Vigil, R., García, R., Villar, E., Oleaga, A., and Vegas, I. Scientific advances regarding the effect of carbonated alkaline waste materials on pozzolanic reactivity. *Journal of Building Engineering*, 2024, *98*, 111423.
23. Zhu, M., Zhai, R., Zhu, M., and He, J. Evaluating Alkali Activation in Magnesium Slag Carbonization and Its Mechanism, *Crystals*, 2024, 14(10), 847.
24. Zhang, L., Zhang, Y., Zhang, F., Liang, H., Niu, D., and Li, H., Mechanical and Ecological Properties of CO2 Curing Magnesium Slag Concrete. *Materials*, *18*(1), 2024, 109.
25. Nawaz, M., Heitor, A., Sivakumar, M., Geopolymers in construction-recent developments, *Construction and Building Materials*, 2020, 260, 120472.
26. Sharma, A., Basumatary, N., Singh, P., Kapoor, K., and Singh, S. P., Potential of geopolymer concrete as substitution for conventional concrete: A review, *Materials Today: Proceedings*, 2022, 57, 1539–1545.
27. Neupane, K., 2016. Fly ash and GGBFS based powder-activated geopolymer binders: A viable sustainable alternative of portland cement in concrete industry, Mechanics of Materials, 103, 110–122.
28. Deb, P. S., Nath, P., and Sarker, P. K., The effects of ground granulated blast-furnace slag blending with fly ash and activator content on the workability and strength properties of geopolymer concrete cured at ambient temperature, *Materials & Design*, 2014, 62, 32–39.
29. Yazıcı, N., Karagöl, F., 2022. Investigation of mechanical and durability properties of fly ash-based and slag-incorporated geopolymer concretes, Journal of the Institute of Science and Technology, 12(3), 1592–1606.
30. Fouad, H. E. E., Serag, M. I., Ragab, A., & Hussein, A. (2025). Mechanical Properties and Temperature Resistance of Fly Ash-Based Geopolymer Concrete. *Mansoura Engineering Journal*, *50*(3), 13.
31. Altundal, M. B., 2019. Mechanical behavior of geopolymer concretes containing ground granulated blast furnace slag and fly ash under 5% sulfuric acid exposure, Master's Thesis.
32. Erdoğdu, Ş., Kurbetci, Ş., Kandil, U., Nayır, S., Nas, M., 2021. Some mechanical and durability properties of blast furnace slag concrete, Hazır Beton, 167.
33. Çakır, Ö., 2006. The effect of ground granulated blast furnace slag on the durability of concrete and reinforced concrete, Master's Thesis.
34. Justnes, H., Martius-Hammer, T. A., 2016. Sustainability – The pioneering role in concrete innovation, Hazır Beton, 23, 77–82.

 doi:10.20944/preprints202512.0868.v1

35. Lu, P., Zhao, Y., Zhang, N., Wang, Y., Zhang, J., Zhang, Y., and Liu, X., Structural characteristics and cementitious behavior of magnesium slag in comparison with granulated blast furnace slag. *Materials,* (2024)., *17*(2), 360.
36. Zhang, S. S., Wang, S., and Chen, X., 2024. Understanding the role of magnesium ions on setting of metakaolin-based geopolymer. *Cement and Concrete Research*, *177*, 107430.
37. Dung, N. T., Hooper, T. J. N., & Unluer, C. 2019, Accelerating the reaction kinetics and improving the performance of Na2CO3-activated GGBS mixes. *Cement and Concrete Research*, *126*, 105927.
38. Nath, P., and Sarker, P. K., 2014, Effect of GGBFS on setting, workability and early strength properties of fly ash geopolymer concrete cured in ambient condition. *Construction and Building materials*, *66*, 163-171.
39. Lee, N. K., and Haeng-Ki Lee. Setting and mechanical properties of alkali-activated fly ash/slag concrete manufactured at room temperature. *Construction and Building Materials* 47 (2013): 1201-1209.
40. Hu, Y., Tang, Z., Li, W., Li, Y., and Tam, V. W., Physical-mechanical properties of fly ash/GGBFS geopolymer composites with recycled aggregates. *Construction and Building Materials*, *226*, (2019). 139-151.
41. Rakhimova, Nailia R., and Ravil Z. Rakhimov., Alkali-activated cements and mortars based on blast furnace slag and red clay brick waste, *Materials & Design* 85 (2015): 324-331.
42. Rakhimova, Nailia R., and Ravil Z. Rakhimov., Alkali-activated cements and mortars based on blast furnace slag and red clay brick waste, *Materials & Design* 85 (2015): 324-331.
43. Chen, C., Gong, W., Lutze, W., Pegg, I. L. and Zhai, J. Kinetics of fly ash leaching in strongly alkaline solutions. *Journal of Materials Science*, *46*(3), (2011), 590-597.
44. Espinosa, A. B., Revilla-Cuesta, V., Skaf, M., Faleschini, F., and Ortega-López, V, Utility of ultrasonic pulse velocity for estimating the overall mechanical behavior of recycled aggregate self-compacting concrete. *Applied Sciences*, *13*(2), (2023). 874.
45. Lu, P., Zhao, Y., Zhang, N., Wang, Y., Zhang, J., Zhang, Y., and Liu, X. Structural characteristics and cementitious behavior of magnesium slag in comparison with granulated blast furnace slag. *Materials*, (2024). *17*(2), 360.
46. Somna, K., Jaturapitakkul, C., Kajitvichyanukul, P., and Chindaprasirt, P., NaOH-activated ground fly ash geopolymer cured at ambient temperature, *Fuel*, 2011, 90(6), 2118-2124.
47. Mikuni, A., Komatsu, R., and Ikeda, K., Dissolution properties of some fly ash fillers applying to geopolymeric materials in alkali solution. *Journal of materials science*, *42*(9), 2007, 2953-2957.
48. Ji, G., Peng, X., Wang, S., Hu, C., Ran, P., Sun, K., and Zeng, L. Influence of magnesium slag as a mineral admixture on the performance of concrete. *Construction and Building Materials*, *295*, 2021, 123619.
49. Lu, P., Zhao, Y., Zhang, N., Wang, Y., Zhang, J., Zhang, Y., and Liu, X., Structural characteristics and cementitious behavior of magnesium slag in comparison with granulated blast furnace slag. Materials, 17(2), 2024, 360.
50. Amini, O., and Ghasemi, M. Laboratory study of the effects of using magnesium slag on the geotechnical properties of cement stabilized soil. *Construction and Building Materials*, 2019, *223*, 409-420.
51. Wei, F., Xiao, H., Zhang, J., He, Z., Cao, X., and Guan, B. Feasibility study of magnesium slag, fly ash, and metakaolin to replace part of cement as cementitious materials. *Buildings*, *14*(12), (2024), 3874.
52. Bernal, S. A., Rodríguez, E. D., Mejía de Gutiérrez, R., Gordillo, M., and Provis, J. L. Mechanical and thermal characterization of geopolymers based on silicate-activated metakaolin/slag blends. *Journal of materials science*, *46*(16), 2011, 5477-5486.
53. Provis, J. L., and Van Deventer, J. S. J. (Eds.)., Geopolymers: structures, processing, properties and industrial applications. Elsevier. 2009.
54. Li, Z., Zhang, W., Wang, R., Chen, F., Jia, X., and Cong, P. (2019). Effects of reactive MgO on the reaction process of geopolymer. *Materials*, *12*(3), 526.
55. Nath, P., and Sarker, P. K. (2014). Effect of GGBFS on setting, workability and early strength properties of fly ash geopolymer concrete cured in ambient condition. *Construction and Building materials*, *66*, 163-171.
56. Provis, J. L., and Van Deventer, J. S. J. (Eds.). (2009). Geopolymers: structures, processing, properties and industrial applications. *Elsevier*.

 doi:10.20944/preprints202512.0868.v1